

# Effect of surface hydroxyl groups on heat capacity of mesoporous silica

## - Supplementary material -

Michal Marszewski,<sup>1</sup> Danielle Butts,<sup>2</sup> Esther Lan,<sup>2</sup> Yan Yan,<sup>3</sup> Sophia C. King,<sup>3</sup> Patricia E. McNeil,<sup>2</sup> Tiphaine Galy,<sup>1</sup> Bruce Dunn,<sup>2</sup> Sarah H. Tolbert,<sup>2,3</sup> Yongjie Hu,<sup>1</sup> Laurent Pilon<sup>1,a)</sup>

<sup>1</sup>*Mechanical and Aerospace Engineering Department, University of California, Los Angeles, Los Angeles, California 90095, USA*

<sup>2</sup>*Department of Materials Science and Engineering, University of California, Los Angeles, Los Angeles, California 90095, USA*

<sup>3</sup>*Department of Chemistry and Biochemistry, University of California at Los Angeles, Los Angeles, California 90095, USA*

<sup>a)</sup>*Author to whom correspondence should be addressed. Electronic mail: pilon@seas.ucla.edu.*

### Nomenclature

$c_p$	specific heat capacity ( $\text{J g}^{-1} \text{K}^{-1}$ )
$\bar{d}_p$	average pore width (nm)
$e$	thermal effusivity ( $\text{J m}^{-2} \text{K}^{-1} \text{s}^{-1/2}$ )
$k$	thermal conductivity ( $\text{W m}^{-1} \text{K}^{-1}$ )
$m$	mass (g)
$n$	number of moles (mol)
$M_{OH}$	molar mass of hydroxyl group ( $M_{OH} = 17 \text{ g mol}^{-1}$ )
$p/p_0$	relative pressure
$S_a$	specific surface area ( $\text{m}^2 \text{g}^{-1}$ )
$V_t$	total pore volume ( $\text{cm}^3 \text{g}^{-1}$ )
$w$	weight fraction

### Greek symbols

$\alpha$	thermal diffusivity ( $\text{m}^2 \text{s}^{-1}$ )
$\phi$	porosity or air volume fraction
$\rho c_p$	volumetric heat capacity ( $\text{J m}^{-3} \text{K}^{-1}$ )
$\rho$	density ( $\text{g cm}^{-3}$ )
$\sigma_{OH}$	surface density of hydroxyl groups ( $\text{mol m}^{-2}$ )

### Subscripts and superscripts

air	refers to air
eff	refers to effective
H <sub>2</sub> O	refers to water
OH	refers to OH groups
SiO <sub>2</sub>	refers to silica
total	refers to entire sample

## Porosity and specific area measurements

Low-temperature nitrogen adsorption–desorption isotherms were measured at  $-196\text{ }^{\circ}\text{C}$  using a surface area and porosity analyzers ASAP 2010 and TriStar II 3020 (Micromeritics Instrument Corp., Norcross, GA, USA). To do so, each sample was degassed in vacuum at  $150\text{--}200\text{ }^{\circ}\text{C}$  for  $20\text{--}24\text{ h}$  prior to measurements. The specific surface area  $S_a$  was calculated using the Brunauer–Emmett–Teller method<sup>1</sup> (BET) based on low-temperature nitrogen adsorption data in the relative pressure  $p/p_0$  range  $0.05\text{--}0.2$ , assuming the cross-sectional area of a nitrogen molecule to be  $0.162\text{ nm}^2$ .<sup>2</sup> The total pore volume  $V_t$  was calculated by converting the volume of nitrogen adsorbed at a relative pressure  $p/p_0 = 0.98$  to the volume of liquid nitrogen assuming the density conversion factor of  $0.0015468$ .<sup>2,3</sup> Then, the porosity  $\phi$  was calculated from the total pore volume  $V_t$  according to<sup>3</sup>

$$\phi = (V_t \rho_{SiO_2}) / (1 + V_t \rho_{SiO_2}). \quad (\text{S1})$$

The micropore volume  $V_{mi}$  was calculated using the  $\alpha_s$  comparative method<sup>3</sup> in the reduced adsorption  $\alpha_s$  range  $0.8\text{--}1.1$  (S1, S3–S8, S10, and S12) or  $0.4\text{--}0.8$  (S2, S9, and S11) and using macroporous silica LiChrospher Si-1000 as a reference.<sup>4</sup> The reduced adsorption  $\alpha_s$  was defined as<sup>3</sup>

$$\alpha_s = a_{ref} / a_{ref,0.4}, \quad (\text{S2})$$

where  $a_{ref}$  is the amount of nitrogen adsorbed on the reference material surface at a given relative pressure  $p/p_0$  and  $a_{ref,0.4}$  is the amount of nitrogen adsorbed at the reference material surface at the relative pressure  $p/p_0 = 0.4$ . In addition, the average pore width  $\bar{d}_p$  was calculated based on the pore size distribution determined using the Kruk–Jaroniec–Sayari (KJS) method<sup>5</sup> based on the Barrett–Joyner–Halenda (BJH) method<sup>6</sup> using (i) the adsorption branch of nitrogen isotherm, (ii) the modified Kelvin equation<sup>5</sup> calibrated for cylindrical pores up to  $19\text{ nm}$  in diameter, and (iii) the statistical film thickness curve derived from the nitrogen adsorption isotherm measured for macroporous silica LiChrospher Si-1000.<sup>4</sup> Note that for cylindrical pores the specific surface area  $S_a$  relates to the average pore width  $\bar{d}_p$  according to<sup>3</sup>

$$S_a = \frac{4V_t}{\bar{d}_p}. \quad (\text{S3})$$

### Specific heat measurements

The effective specific heat capacity  $c_{p,eff}$  of all samples S1–S12 was measured at 25 °C using a DSC 8000 heat-flow differential scanning calorimeter (PerkinElmer Inc., Waltham, MA, USA) and a step-scan option. First, the effective specific heat capacity  $c_{p,eff,as}$  of the as-synthesized sample was measured. The as-synthesized samples were allowed to (i) equilibrate the amount of physically-adsorbed water and (ii) regenerate the surface OH groups before the measurement. Second, the sample was degassed at 160 °C in the calorimeter under dry nitrogen flow to ensure that the physically adsorbed water was removed but the surface OH groups remained.<sup>7</sup> Next, the apparent specific heat capacity  $c_{p,app,deg}$  of the degassed sample (calculated per original mass of the sample) was measured. Then, the water weight fraction  $w_{H_2O}$  present in the as-synthesized sample was calculated as

$$w_{H_2O} = (c_{p,eff,as} - c_{p,eff,deg})/c_{p,H_2O}, \quad (S4)$$

where  $c_{p,H_2O}$  is the specific heat capacity of water taken as  $c_{p,H_2O} = 4.184 \text{ J g}^{-1} \text{ K}^{-1}$ . Finally, the effective specific heat capacity  $c_{p,eff}$  of mesoporous silica sample was calculated by correcting the apparent specific heat capacity  $c_{p,app,deg}$  of the degassed sample for the mass lost due to water removal as

$$c_{p,eff} = c_{p,app,deg}/(1 - w_{H_2O}), \quad (S5)$$

Each measurement was corrected with a baseline run and for the mass difference between the sample pan and the reference pan.

### FTIR Transmission spectra

Fourier-transform infrared (FTIR) transmission spectra were collected on a FT/IR-6100 spectrometer (Jasco, Germany) in a 4000–400  $\text{cm}^{-1}$  range with a 4  $\text{cm}^{-1}$  spectral resolution. Each sample was ground, mixed with ground KBr, and pressed into a pellet before the transmission measurement. The absorption band at ca. 2350  $\text{cm}^{-1}$  corresponding to atmospheric  $\text{CO}_2$  was removed for clarity.

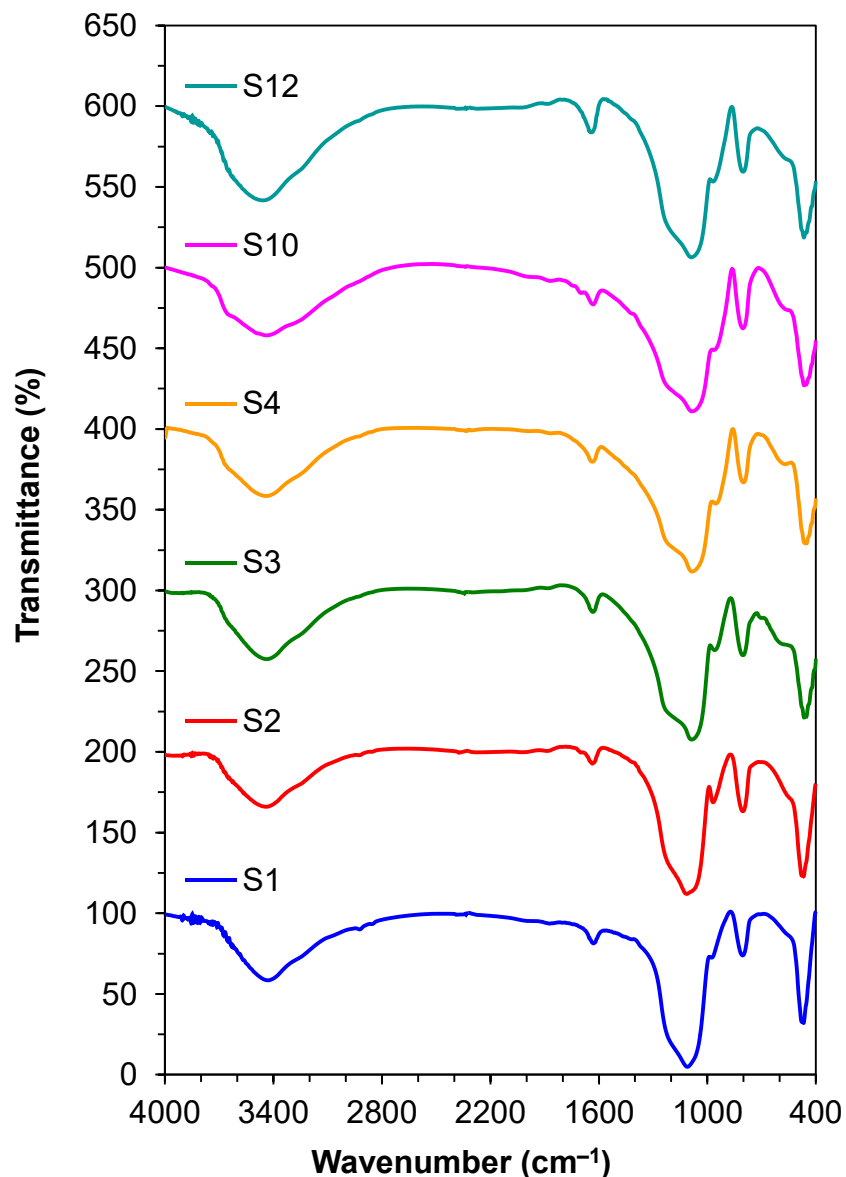


FIG. S1. Fourier-transform infrared transmittance spectra of mesoporous nanoparticle-based silica samples S1 and S2, mesoporous sol-gel silica samples S3 and S4, and mesoporous ambigel silica samples S10 and S12. Patterns shifted upwards for clarity by 0, 100, 200, 300, 400, and 500 %, respectively.

All FTIR spectra of representative nanoparticle-based, sol-gel, and ambigel mesoporous silica samples (Fig. S1) featured a broad absorption band between 3700 and 3000  $\text{cm}^{-1}$  corresponding to O–H stretching vibrations of OH surface groups and OH groups in water physically adsorbed on the materials' surface.<sup>8–10</sup> In addition, all samples featured an absorption band at 1630–1620  $\text{cm}^{-1}$  corresponding to H–O–H bending vibrations of physisorbed water.<sup>8–10</sup> Multiple absorption bands at 1200–1000, 970–940, 800, 580–550, and 470–450  $\text{cm}^{-1}$  were all ascribed to vibrations of  $\text{SiO}_2$

network: Si–O–Si asymmetric stretching, Si–OH in-plane stretching, Si–O symmetric stretching, Si–O stretching, and O–Si–O bending vibrations, respectively.<sup>8–10</sup> Finally, no absorption bands in the range 3000–1350 cm<sup>-1</sup>, corresponding to organic molecules, were detected. Therefore, the prepared samples did not contain organic residues that could otherwise affect the measured effective specific heat capacity  $c_{p,eff}$ .

### **Powder X-ray diffraction**

In addition, powder X-ray diffractograms were collected on a MiniFlex II powder X-ray diffractometer (Rigaku, The Woodlands, TX, USA) using Cu K $\alpha$  radiation (30 kV, 15 mA,  $\lambda = 1.5406 \text{ \AA}$ ). All scans were taken in the  $2\theta$  range 10.00°–80.00° with a 0.02° step size. Fig. S2 (on page S6) shows X-ray diffraction patterns of the same selected mesoporous silica samples. It indicates that the diffraction patterns were featureless except for a broad hump between  $2\theta$  equals to 10° and 40°, indicating that the mesoporous SiO<sub>2</sub> samples were amorphous.<sup>11</sup>

### **Reference**

- <sup>1</sup> S. Brunauer, P.H. Emmett, and E. Teller, *J. Am. Chem. Soc.* **60**, 309 (1938).
- <sup>2</sup> M. Kruk and M. Jaroniec, *Chem. Mater.* **13**, 3169 (2001).
- <sup>3</sup> J. Rouquerol, F. Rouquerol, P. Llewellyn, G. Maurin, and K.S.W. Sing, *Adsorption by Powders and Porous Solids: Principles, Methodology and Applications*, 2<sup>nd</sup> Edition (Academic Press, Amsterdam, 2013).
- <sup>4</sup> M. Jaroniec, M. Kruk, and J.P. Olivier, *Langmuir* **15**, 5410 (1999).
- <sup>5</sup> M. Kruk, M. Jaroniec, and A. Sayari, *Langmuir* **13**, 6267 (1997).
- <sup>6</sup> E.P. Barrett, L.G. Joyner, and P.P. Halenda, *J. Am. Chem. Soc.* **73**, 373 (1951).
- <sup>7</sup> L.T. Zhuravlev, *Langmuir* **3**, 316 (1987).
- <sup>8</sup> R.F.S. Lenza and W.L. Vasconcelos, *Mater. Res.* **4**, 189 (2001).
- <sup>9</sup> R. Al-Oweini and H. El-Rassy, *J. Mol. Struct.* **919**, 140 (2009).
- <sup>10</sup> C. Knöfel, C. Martin, V. Hornebecq, and P.L. Llewellyn, *J. Phys. Chem. C* **113**, 21726 (2009).
- <sup>11</sup> H. Hamdan, M.N.M. Muhid, S. Endud, E. Listiorini, and Z. Ramli, *J. Non-Cryst. Solids* **211**, 126 (1997).

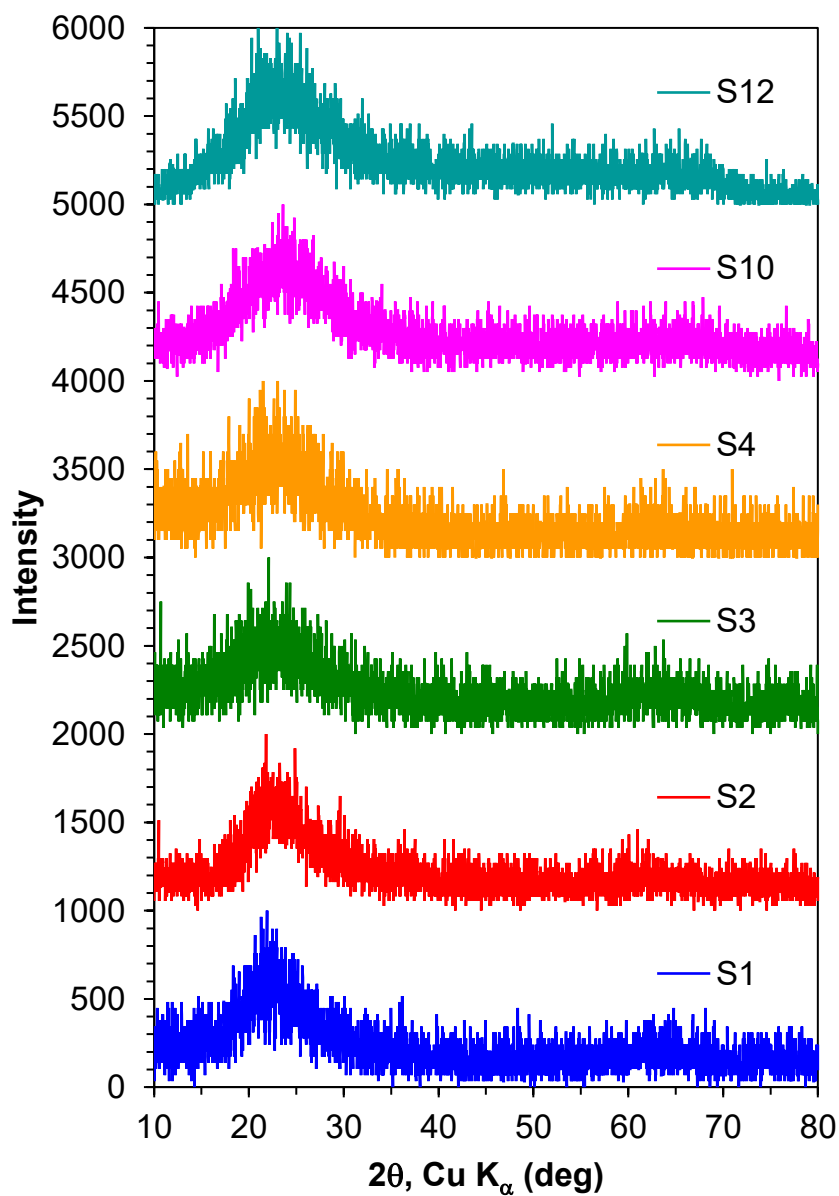


FIG. S2. Powder X-ray diffraction patterns of mesoporous nanoparticle-based silica samples S1 and S2, mesoporous sol-gel silica samples S3 and S4, and mesoporous ambigel silica samples S10 and S12. Patterns shifted upwards for clarity by 0, 1000, 2000, 3000, 4000, and 5000, respectively.